Synthesis, Optical Properties, and Aggregation Behavior of a Triad System Based on Perylene and Oligo(*p*-phenylene vinylene) Units

Asha Syamakumari, Albertus P. H. J. Schenning, and E. W. Meijer*[a]

Abstract: A donor-acceptor-donor triad molecule with a perylene bisimide derivative as electron acceptor, and an oligo(*p*-phenylene vinylene) (OPV) derivative as electron donor was synthesized (**OPV-PERY-OPV**). The structure of the triad was characterized by ^{1}H and ^{13}C NMR spectroscopy, size-exclusion chromatography (SEC), and MALDI-TOF spectrometry. Absorbance spectra and CD spectroscopic measurements of the triad molecule indicated the formation of aggregates in solvents such as toluene, chloroform, and tetrachloroethane, whereas it was present in the molecularly dissolved state in THF. The ^{1}H NMR spectra of the molecule in chloroform had, unexpectedly, four doublet peaks for the perylene protons, instead of the two doublets that is generally seen in *N*,*N*′-substituted perylene molecules. To understand the aggregation behavior and the splitting of the signals in the ^{1}H NMR spectra, a simple model compound was synthesized, in which the OPV units were replaced by phenyl groups (**Ph-PERY-Ph**). ^{1}H NMR spectra in $CDCl_3$ and tetrachloroethane again had four doublet peaks for the perylene protons, whereas in THF the perylene protons gave only a single peak. NOE and COSY spectroscopy were used to assign the peaks to their corresponding perylene protons. UV/Vis and CD spectroscopic measurements indicated that, similar to the **OPV-PERY-OPV** triad molecule, the model compound **Ph-PERY-Ph** was also present in the aggregated form in solvents such as toluene, chloroform, and tetrachloroethane, and in the molecularly dissolved state in THF. IR measurements of the model molecule in the first set of solvents indicated carbamate bond (−OCO−NH−)-induced intermolecular hydrogen bonding, whereas in THF, the molecule was mostly present in the free form. CPK models with a dimeric structure, in which two perylene molecules are held together by intermolecular hydrogen bonding with the perylene core shifted slightly with respect to one another, could account for the optical properties and the observation of the four different peaks in the ^{1}H NMR spectra in polar solvent. Temperature-dependent ^{1}H NMR spectroscopic, UV/Vis, and CD measurements indicated that the transition from the aggregated to the molecularly dissolved state took place at higher temperatures. The electrochemical studies indicated that **OPV-PERY-OPV** was both *p*- and *n*-dopable, whereas **Ph-PERY-Ph** was only *n*-dopable. Cyclic voltammetry measurements of **Ph-PERY-Ph** in THF had two reduction peaks corresponding to the reduction of the perylene core to the monoanion and dianion, respectively. In dichloromethane, however, an additional reduction peak at lower potential was observed. This new reduction peak might arise from the hydrogen-bonded species.

Keywords: donor-acceptor systems · hydrogen bonds · oligo(*p*-phenylene vinylene) · perylene dyes · supramolecular chemistry

Introduction

Solar cells containing conjugated organic molecules as the electron- and hole-transporting layer are an important area of current interest. There have been various designs of the solar cell that have made use of a wide variety of organic molecules and with different architecture of the cell.[1] Cells with an active layer consisting of covalently linked donor and acceptor units are one of the most promising.[2] These diads have the advantage of a large interfacial area between the donor and acceptor parts, and one can attain better control over the morphology. Supramolecular organization in these systems can lead to separate stacks of the donor and acceptor and to well-defined electron- and hole-transport pathways.[3] Hydrogen bonding is an important tool that has been used to attain supramolecular organization of the donor and acceptor parts.[4]

Perylene bisimides represent one of the most thoroughly studied classes of organic semiconductors with a variety of different structures,[5] with possible applications such as fluorescent solar collectors,[6] photovoltaic devices,[7] dye lasers,[8] molecular switches.[9] These dyes have outstanding chemical, thermal, and photochemical stability. They are highly absorbing in the visible to NIR region ($\varepsilon \approx 10^5\,\mathrm{M^{-1}\,cm^{-1}}$)

[a] Prof. Dr. E. W. Meijer, Dr. Asha Syamakumari, Dr. A. P. H. J. Schenning
Laboratory of Macromolecular and Organic Chemistry
Eindhoven University of Technology
P.O. Box 513, 5600 MB Eindhoven (The Netherlands)
Fax: (+31) 40-2473101

and emit fluorescence with quantum yields near unity.[10] Perylene bisimides are potential candidates as electron-accepting materials in organic photovoltaic solar cells.[11] Very recently, MacKenzie et al. reported the self-organization property of a room temperature discotic liquid crystalline hexabenzocoronene in combination with a crystalline perylene derivative to obtain an efficient photodiode.[12] X-ray structural analysis of several perylene tetracarboxylic acid diimides has revealed a planar perylene diimide core with bent side chains and that they pack in stacks.[13] The mutual arrangement of neighbors in the stacks is dependent on the different substituents which determine the longitudinal and transverse shifting on the perylene π systems. In solution these dyes have a tendency to aggregate[14] into J- or H-type aggregates.[15]

Herein, we report the synthesis of a donor-acceptor-donor triad system with perylene as an electron acceptor, and oligo(*p*-phenylene vinylene) (OPV) units as electron donors. The OPV unit was provided with chiral side chains, and the spacer connecting the OPV and perylene unit also had a chiral side chain to enable aggregation studies by circular dichroism (CD) spectroscopy. The molecule was found to form aggregates in solvents such as toluene and chloroform. To have a simple system for understanding the aggregation behavior, a model compound was synthesized with phenyl rings instead of the OPV units. IR measurements on the model molecule revealed the presence of intermolecular hydrogen bonding induced by the carbamate linkage (−OCO−NH−). A dimeric structure has been proposed for the aggregate, in which two perylene molecules are held together by intermolecular hydrogen bonds.

Results and Discussion

Synthesis: The structures of both the molecules are shown in Scheme 1. The triad molecule **OPV-PERY-OPV** was synthesized by coupling the isocyanate OPV derivative **3a** with **4** by using dibutyltin dilaurate as catalyst. The model molecule **Ph-PERY-Ph** was synthesized by coupling phenyl isocyanate **3b** with **4** under similar conditions as those for the OPV-based triad molecule. Both compounds were fully characterized by ^{1}H, ^{13}C NMR spectroscopy, size-exclusion chromatography (SEC), and MALDI-TOF mass spectrometry. The SEC analysis had single peaks for both compounds. As expected, the elution time of **Ph-PERY-Ph** was longer than that for **OPV-PERY-OPV**. The molecular ion peak (*m/z* 3236 for **OPV-PERY-OPV** and *m/z* 829 for **Ph-PERY-Ph**) and the sodium ion peak (*m/z* 3259 for **OPV-PERY-OPV** and *m/z* 851 for **Ph-PERY-Ph**) obtained in the MALDI-TOF spectra are shown in Figure 1. The intensity of the molecular ion peak for **Ph-PERY-Ph** is much smaller relative to its sodium ion peak. For **Ph-PERY-Ph**, a very small peak corresponding to twice the mass of the molecule was also observed at 1704 (Figure 1 inset).

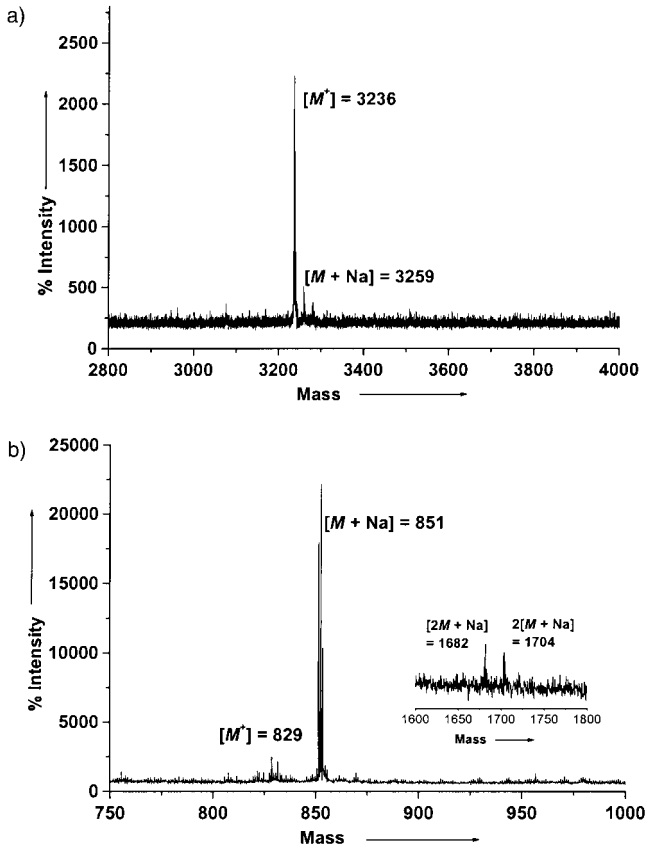

Figure 1. MALDI-TOF spectra: a) **OPV-PERY-OPV**; b) **Ph-PERY-Ph**. Inset: expanded region showing the dimer.

Thermal characteristics: The thermal characteristics of **OPV-PERY-OPV** were determined by using differential scanning calorimeter (DSC, scan rate 40 K min^{-1}). In the first heating cycle of the DSC scan (data not shown), a melting peak was observed. However, no transitions were observed in the first

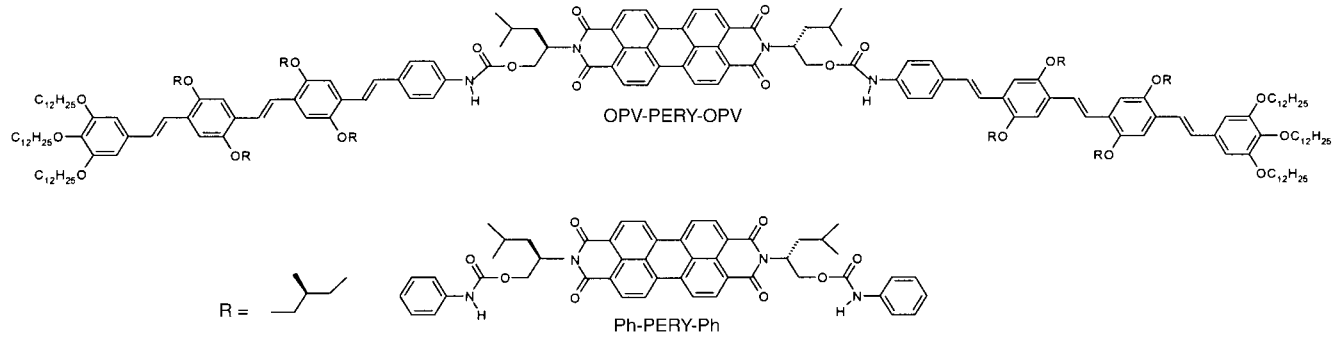

Scheme 1.

0947-6539/02/0815-3354 $ 20.00+.50/0 *Chem. Eur. J.* **2002**, *8*, No. 15

cooling scan or in the following second and third heating and cooling cycles. Both molecules were further investigated with polarization microscopy. On heating, **OPV-PERY-OPV** went into a viscous state before isotropization, and while cooling a glassy state was formed which did not crystallize. On the other hand, **Ph-PERY-Ph** melted on heating to 240 °C and recrystallized on cooling.

It was rather surprising that with the 3,4,5-tridodecyloxyphenyl tails, **OPV-PERY-OPV** did not show any liquid crystalline behavior.[15] However, similar behavior has been reported in the literature for some polyoxyethylene-substituted perylene diimides, in which the isotropic sample froze when cooled to room temperature into an apparently isotropic glassy state that crystallized only very slowly.[16]

^{1}H NMR analysis and IR studies: The ^{1}H NMR of both molecules were recorded in $CDCl_3$ and their expanded aromatic regions are given in Figure 2. The arrows indicate the perylene protons and the asterisks indicate the solvent peaks in the spectra. The peaks at $\delta = 9.3$ ppm (Figure 2a) and $\delta = 9.1$ ppm (Figure 2b) were assigned to the N–H protons based on deuterium exchange measurements performed by adding a few drops of D_2O to a solution of the sample in $CDCl_3$. The eight protons of perylene appear as four doublets in the proton NMR spectra at $\delta = 7.6 - 8.8$ ppm. This was rather unexpected as most of the perylene derivatives gave only two peaks: one set for the two inner ring protons and another set for the two outer ring protons.[15]

COSY and NOE experiments were carried out on **Ph-PERY-Ph** in $CDCl_3$ to assign the peaks to their corresponding perylene protons. The plot of the COSY cross-peaks indicated strong cross-coupling between peaks 1 and 3 and between peaks 2 and 4 (Figure 3). NOE experiments revealed an NOE effect between the peaks marked 1 and 2 ($\delta = 8.64$ and 8.16 ppm, respectively). Therefore, peaks 1 and 2 were assigned to the two inner protons of the perylene ring. This NOE effect between protons 1 and 2 is an indication that they are not chemically equivalent. Since COSY indicated cross-coupling of peak 1 with 3 and peak 2 with 4, peak 3 was assigned to the outer proton next to 1 and 4 was assigned as the one next to 2 (Scheme 2).

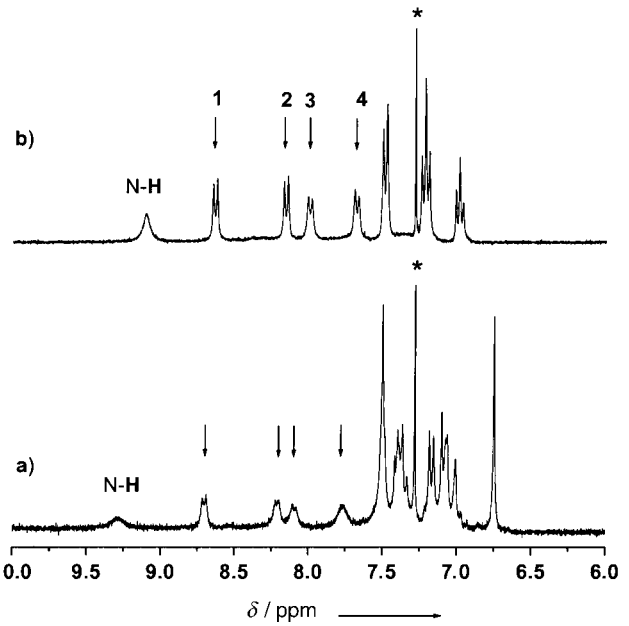

Figure 2. ^{1}H NMR spectra of a) **OPV-PERY-OPV** and b) **Ph-PERY-Ph** in $CDCl_3$.

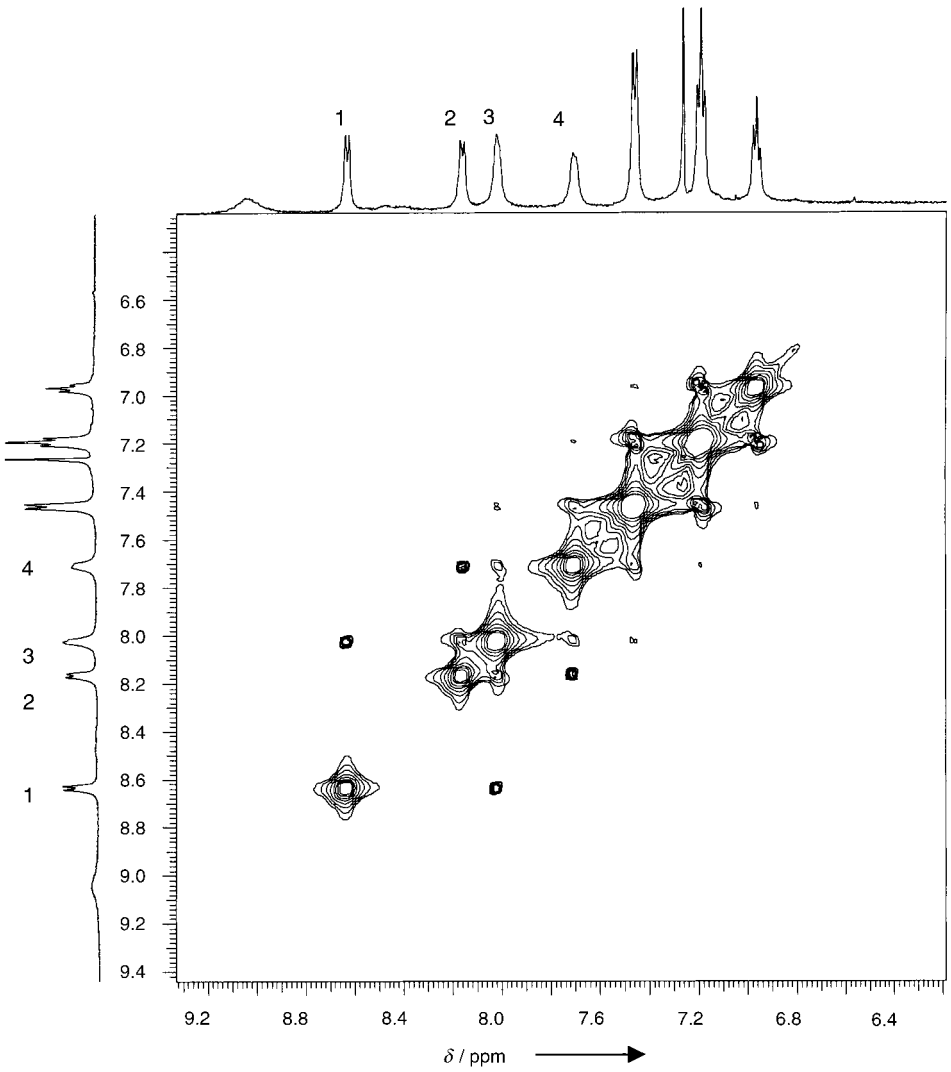

Figure 3. COSY ^{1}H NMR spectrum of **Ph-PERY-Ph** in $CDCl_3$.

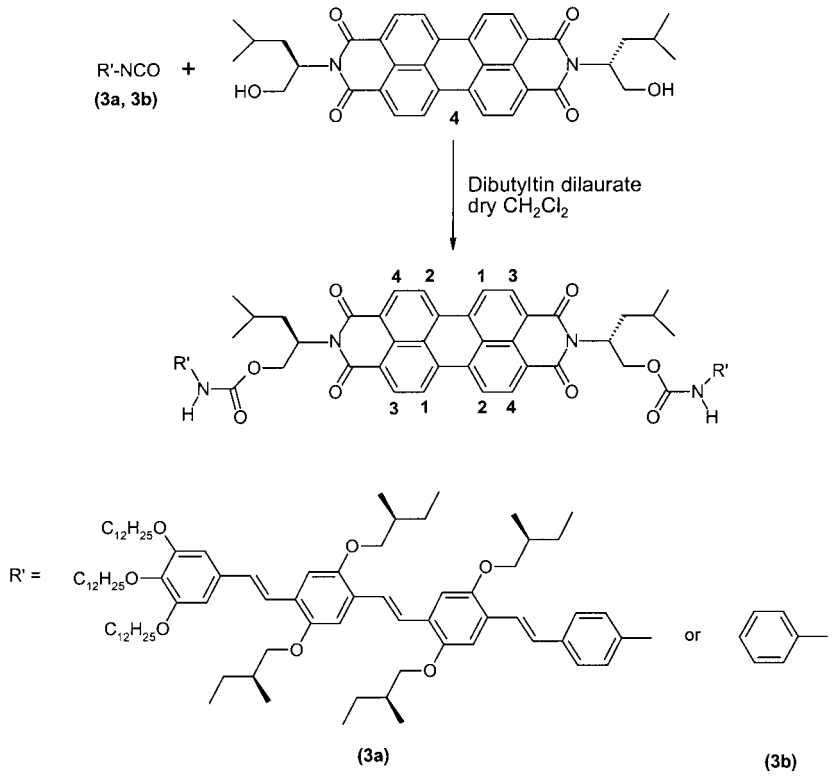

Scheme 2.

^{1}H NMR spectra of a similar molecule with a simple hexyl spacer instead of the carbamate linkage (−NH−COO−) between the phenyl ring and the branched spacer of the perylene moiety, gave only two peaks for the perylene protons. This indicated that hydrogen bonding induced by the carbamate group was presumably responsible for the unusual splitting pattern of the perylene protons. Hydrogen bonding, whether intermolecular or intramolecular, can lead to restricted rotation about the N−C* (asymmetric center) bond, which in turn can give rise to two possible atropisomers: one in which the spacer segments (e.g., for the −OCO−NH− linkage) are opposite to each other (*trans* form), and another in which they are on the same plane of the perylene core (*cis* form). CPK models indicate that only the latter atropisomer can explain the occurrence of the strong NOE effect.

The ^{1}H NMR spectra of **Ph-PERY-Ph** were also measured in [D_8]THF (Figure 4) and in [D_2]TCE (Figure 5, the bottom-most spectra). In TCE, the splitting pattern of the perylene protons is very much similar to that in $CDCl_3$. In THF, on the other hand, they appear as a single peak. The relative intensity of the single perylene peak matched perfectly with that of the phenyl protons. The observation of only a single peak for the perylene protons may be due to the fact that they become coincident in THF. A temperature-dependent measurement in [D_2]TCE of **Ph-PERY-Ph** (Figure 5) indicated that the four peaks of the perylene protons coalesced at around 75 °C to form two peaks at higher temperature. At temperatures above 75 °C, the hydrogen bonding is broken and the usual NMR spectrum is observed. In solvents such as THF, which does not favor hydrogen bonding, the unusual splitting pattern is not observed.

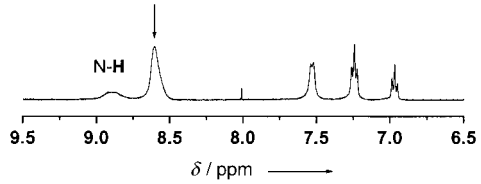

Figure 4. ^{1}H NMR spectrum of **Ph-PERY-Ph** in [D_8]THF.

IR spectroscopy is a valuable tool for hydrogen bond characterization and it has been used to distinguish between hydrogen-bonded and free N−H, and carbonyl stretching vibrations of the carbamate linkage.[17] IR spectra were recorded for **Ph-PERY-Ph** in toluene, chloroform, and THF. The expanded region of the N−H stretching vibration in these solvents is given in Figure 6. The two bands at higher wavenumbers (3690 and 3604 cm^{-1} in chloroform, 3679 and 3595 cm^{-1} in toluene, and 3572 and 3503 cm^{-1} in THF) were assigned to the free antisymmetric and symmetric stretching vibrations of the N−H group in the carbamate linkage, respectively.[17] The band at lower wavenumber (3331 cm^{-1} in chloroform, 3324 cm^{-1} in toluene, and

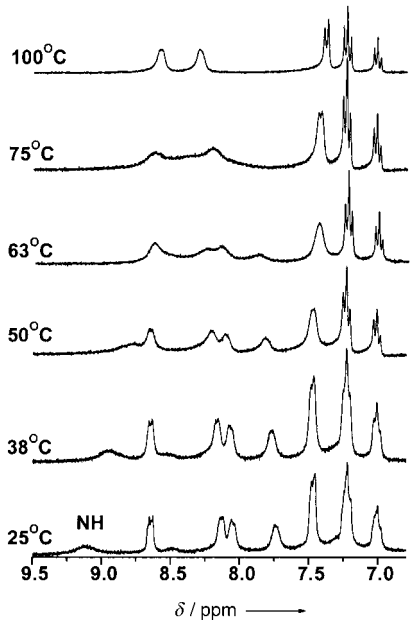

Figure 5. Variable-temperature ^{1}H NMR measurement of **Ph-PERY-Ph** in [D_2]TCE.

0947-6539/02/0815-3356 $ 20.00+.50/0 *Chem. Eur. J.* **2002**, *8*, No. 15

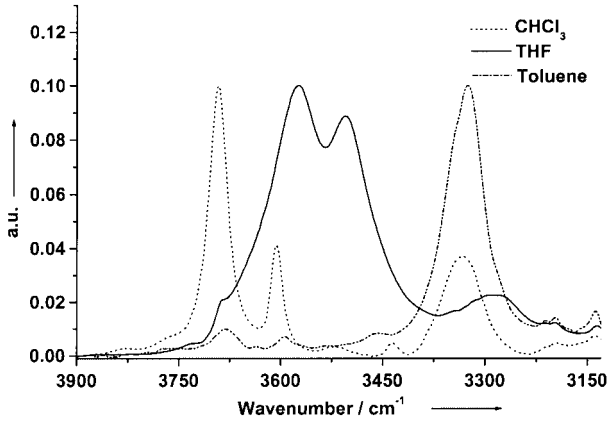

Figure 6. IR measurements of **Ph-PERY-Ph** in $CHCl_3$, THF, and toluene (concentrations were maintained at 10^{-3} M).

3281 cm^{-1} in THF) were assigned to the hydrogen-bonded N–H stretching vibration. By comparing the intensities of the hydrogen-bonded and free amide peaks, it can be seen that in toluene the carbamate hydrogen is mostly present in the hydrogen-bonded state, whereas in THF it is mostly present in the free form. In chloroform, the amount of the hydrogen-bonded and free N–H species is almost equal. To confirm the nature of the hydrogen bonding involved (i.e., inter- or intramolecular), a concentration-dependent measurement was carried out in toluene (Figure 7). The inset in Figure 7

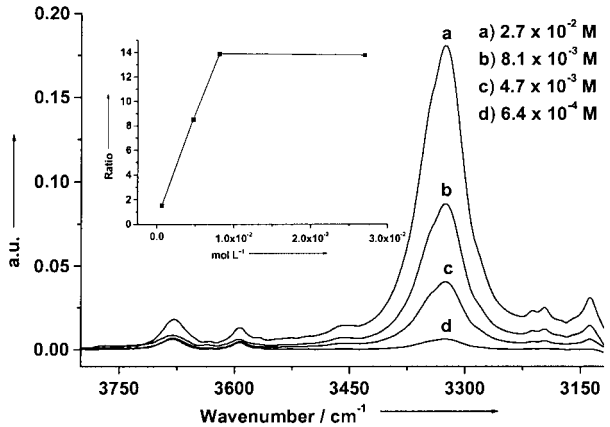

Figure 7. Variable-concentration IR measurements of **Ph-PERY-Ph** in toluene. Inset: plot of ratio of intensities of hydrogen-bonded to non-hydrogen-bonded peaks with concentration.

shows the plot of the ratio of the intensity of the hydrogen-bonded N–H band to that of one of the non-hydrogen-bonded bands as a function of concentration. The ratio is concentration dependent, which is characteristic of intermolecular hydrogen bonding. At higher concentrations, the peak ratio remained invariant with concentration. A dimeric structure can be proposed for the aggregate, in which two perylene molecules are brought together by intermolecular hydrogen bonding, based on the observations from the IR measurements and the fact that at higher concentrations the solution does not indicate any polymeric (e.g., viscous) behavior. A CPK model of the dimer indicates that it is possible to obtain the intermolecularly hydrogen-bonded structure if the two perylene molecules are slightly shifted with respect to one another and not directly on top of each other (Scheme 3). The dimeric structure explains the NMR (COSY, NOE, and proton NMR) experiments and is also in agreement with the IR and UV data.

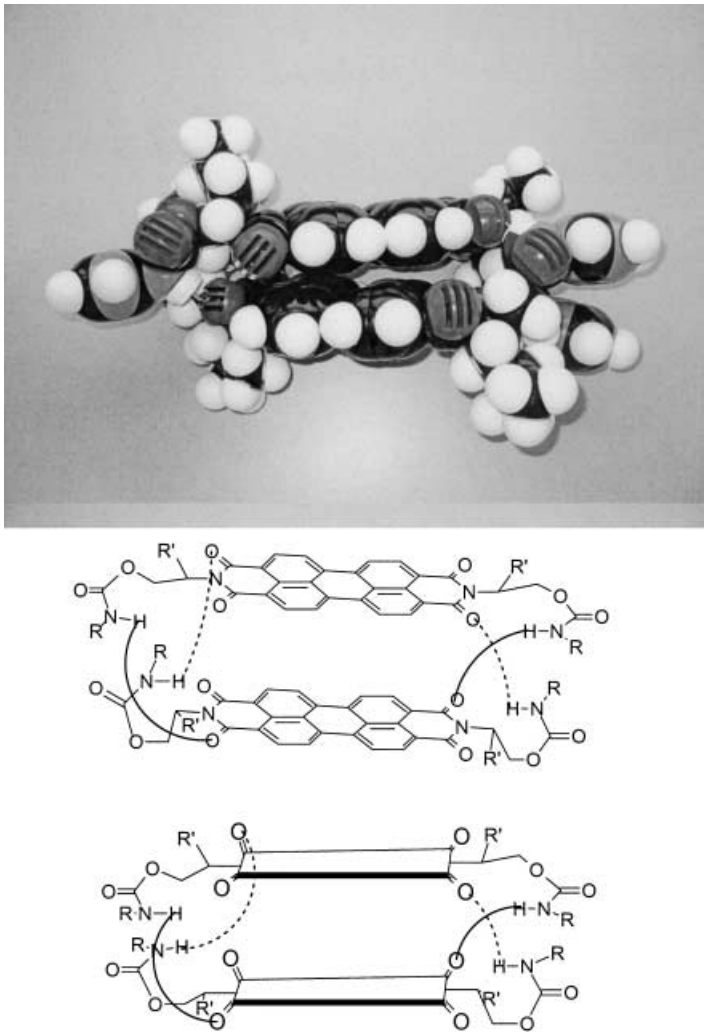

Scheme 3.

The MALDI-TOF spectra of **Ph-PERY-Ph** has mass peaks corresponding to dimers, which although of low intensity can also be assumed to give further evidence for the existence of dimeric molecules. Although it can be argued that there is the possibility of the formation of such species in the gas-phase during the MALDI-TOF measurement, the fact that they are formed nonetheless shows the tendency of the molecules to exist as dimers.

UV/Vis measurements: The UV/Vis spectrum of **OPV-PERY-OPV** was recorded in various solvents (Figure 8). The UV absorbance in solution has a main band centered at around 435 nm, a shoulder at 486 nm, and another peak at 526 nm. The peak at 435 nm corresponds to the $\pi-\pi^*$ transition of the OPV, while the ones at 486 and 526 nm correspond to the perylene unit. The UV/Vis spectrum in toluene and chloroform had a shoulder at higher wavelength,

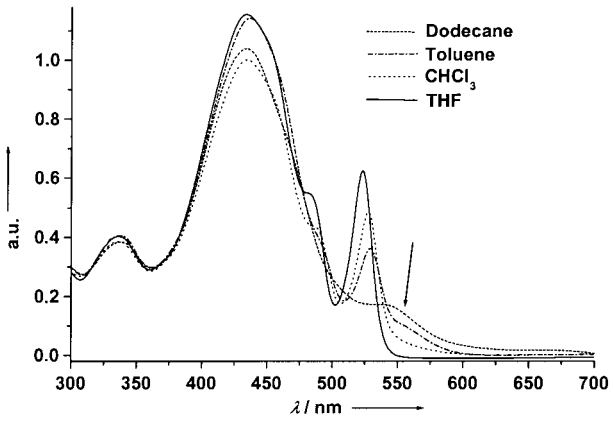

Figure 8. UV/Vis spectra of **OPV-PERY-OPV** in various solvents.

(554 nm, highlighted by the arrow in Figure 8), which indicates aggregation.[15, 18] Similar to the observation in **OPV-PERY-OPV**, in toluene, TCE, and chloroform, **Ph-PERY-Ph** has an additional shoulder at wavelengths above 550 nm as a result of aggregation. Since the aggregation behavior was quite prominent in toluene, a variable-temperature UV/Vis measurement was carried out in this solvent (Figure 9). As the temperature was decreased from 90 °C to

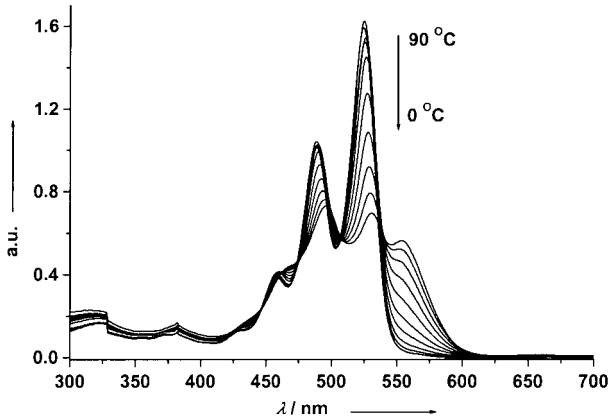

Figure 9. Variable-temperature UV/Vis spectra of **Ph-PERY-Ph** in toluene.

0 °C, the shoulder at 554 nm increased while the peak at 524 nm decreased in intensity. A plot of absorbance at 554 nm versus temperature (not shown) revealed that at around 60 °C the molecule was molecularly dissolved. This value is slightly lower than that from the variable-temperature proton NMR measurements in TCE (Figure 5), in which the four peaks corresponding to the eight perylene protons merged to form two at around 75 °C. The transition from aggregated species to molecularly dissolved species takes place over a broad temperature range. At 0°C, monomeric species are still present because the absorption at $\lambda = 554$ nm has not reached its maximum. Therefore, the temperature at which only monomers are present will not change dramatically if the concentration is increased by three orders of magnitude as used in the NMR experiments.

Circular dichroism (CD) measurements: CD measurements were carried out for **OPV-PERY-OPV** in various solvents (Figure 10). In toluene a bisignate signal is present that

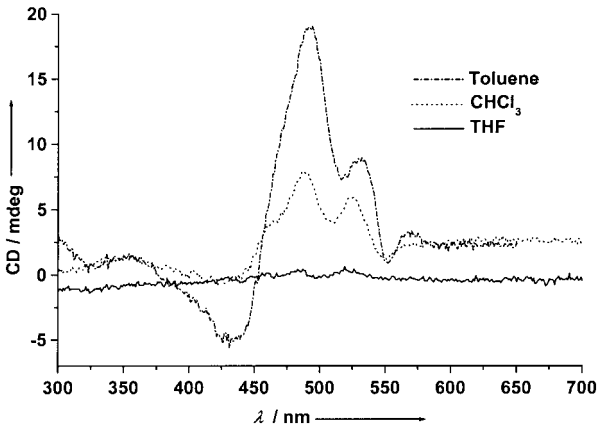

Figure 10. Circular dichroism (CD) measurements of **OPV-PERY-OPV** in various solvents (concentrations were maintained at $10^{-4}-10^{-5}$ M).

corresponds to the π-conjugated segment of the OPV part in the UV/Vis absorption spectra. In chloroform, only a positive CD effect is present, whereas in THF there is no signal at all. CD measurements for **Ph-PERY-Ph** were also carried out in various solvents (Figure 11). In toluene, tetrachloroethane, and chloroform, a bisignate CD signal exists corresponding to the aggregation peak in the UV/Vis absorption spectra. As in the case of the triad molecule, there is similarly no CD signal observed here in THF. The UV/Vis and CD measurements indicate that both the molecules are present in the molecularly dissolved form in THF, but in solvents such as toluene, tetrachloroethane, and chloroform, aggregation occurs.

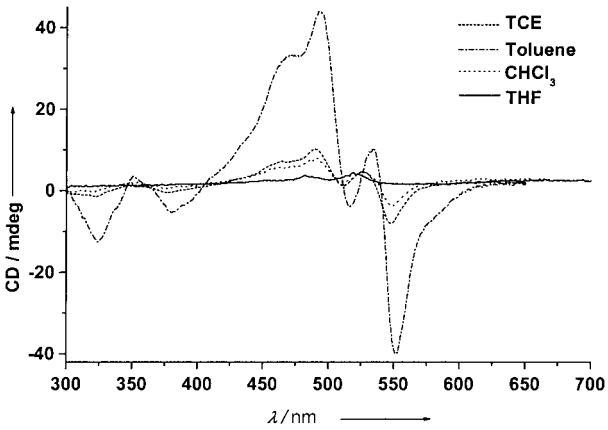

Figure 11. Circular dichroism (CD) measurements of **Ph-PERY-Ph** in various solvents (concentrations were maintained at $10^{-4}-10^{-5}$ M).

Electrochemical properties: The electrochemical properties of both the molecules were investigated using cyclic voltammetry (CV).

The redox behavior of **OPV-PERY-OPV** in dichloromethane (Table 1) indicates both reversible oxidative and reductive processes with oxidation peaks at 0.45 and 0.23 V

0947-6539/02/0815-3358 $ 20.00+.50/0 *Chem. Eur. J.* **2002**, *8*, No. 15

Table 1. Electrochemical properties of **OPV-PERY-OPV** and **Ph-PERY-Ph**.

Sample	E_{pc}[a]	E_{pa}[a]	E_{pc}	E_{pa}	E_{pc}	E_{pa}
OPV-PERY-OPV (CH_2Cl_2)	−1.03	−1.00	−1.33	−1.23	–	–
Ph-PERY-Ph (CH_2Cl_2)	−0.91	−0.84	−1.15	−1.09	−1.40	−1.26
Ph-PERY-Ph (THF)	−1.06	−1.01	−1.37	−1.33	–	–

[a] E_{pa} and E_{pc} stand for anodic and cathodic peak potential respectively.

(versus Fc/Fc^+) of the OPV moiety, and reduction peaks at −1.02 and −1.28 V corresponding to the reduction of the monoanion and the dianion of the perylene moiety. The last of these corresponds very well with the literature values for the perylene bisimide derivative (−1.01, −1.35 V versus Fc/Fc^+).[15]

Figure 12 shows the CV curves of **Ph-PERY-Ph** in dichloromethane and THF. **Ph-PERY-Ph** has only a reduction (*n*-doping) wave in both solvents. In THF, its behavior is similar to that of other perylene bisimide derivatives known in the literature, with two reversible reduction peaks observed at −1.03 and −1.35 V. Surprisingly, when the CV was recorded in dichloromethane, an additional peak appeared at a much lower reduction potential (−0.88 V) than that of the first peak at −1.06 V corresponding to the measurement in THF. The other two reduction peaks were observed at −1.12 and −1.33 V, respectively. The appearance of this new peak, (which is not present in **OPV-PERY-OPV** in CH_2Cl_2) might be rationalized based on the information from the IR data for **Ph-PERY-Ph** recorded in CH_2Cl_2. IR spectra indicated the presence of both hydrogen-bonded and non-hydrogen-bonded species in CH_2Cl_2, whereas only the non-hydrogen-bonded species was present in THF. It may be assumed that in dichloromethane, the hydrogen-bonded species gets reduced at a lower reduction potential than the "free" species, since in the former case the electron density at the perylene core is much lower. The strength of the hydrogen bonding in **OPV-PERY-OPV** is much lower than that in the model molecule (**Ph-PERY-Ph**) in solvents such as toluene and chloroform, as can be seen from the smaller 'aggregation' peak in the UV spectra of the former in these solvents.

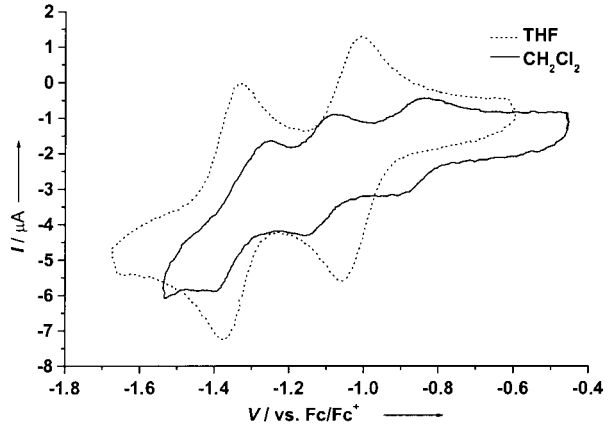

Figure 12. Cyclic voltammograms (CV) of **Ph-PERY-Ph** in various solvents.

Fluorescence measurements: Fluorescence spectra (not shown) were recorded for the **OPV-PERY-OPV** molecule in solvents of varying polarity such as benzonitrile, *ortho*-dicholorobenzene, and toluene, at the excitation wavelength of OPV (445 nm) and perylene (530 nm). In all these solvents, the emission of both the perylene and the OPV fluorescence were completely quenched, indicating an efficient electron transfer process occurring from OPV to perylene. A photo-induced absorption spectra (PIA) was recorded for a thin film of **OPV-PERY-OPV** at 458 nm excitation. The specific absorptions of the $OPV4^{+\cdot}$ radical cation (0.76 and 1.93 eV) and absorptions of the perylene bisimide radical anion (1.26, 1.52, and 1.70 eV) were observed.

The fluorescence spectra of the **Ph-PERY-Ph** molecule were also recorded in the same set of solvents. In THF, the fluorescence excitation spectra matched well with the absorption spectra and there was good mirror-image symmetry between the absorption and fluorescence spectra. The fluorescence maxima were exactly identical to those reported in the literature for similar *N*,*N*′-substituted perylene bisimides and were found at 537, 576, and 628 nm.[19] Figure 13 gives the fluorescence of spectra **Ph-PERY-Ph** in toluene. If excited at $\lambda_{ex} = 461$ nm, a fluorescence spectrum similar to that of THF was observed. However, when excited at $\lambda_{ex} = 556$ nm which correspond to the absorption of the aggregated species only, a new fluorescence band appeared at $\lambda_{em} = 611$ nm.

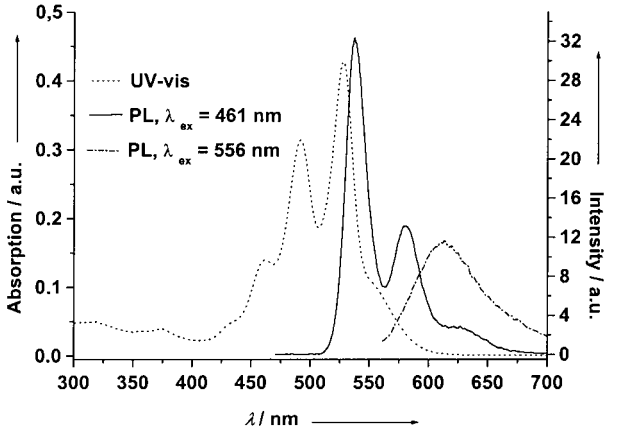

Figure 13. UV/Vis (dotted line) and fluorescence spectra (straight line $\lambda_{ex} = 461$ nm and broken line $\lambda_{ex} = 556$ nm) of **Ph-PERY-Ph** in toluene.

Conclusion

Two perylene bisimide molecules, **OPV-PERY-OPV** and **Ph-PERY-Ph**, with chiral substituents on the imide nitrogen were synthesized. ^1H NMR spectra in chloroform and tetrachloroethane had four doublets for the perylene protons instead of the normal two doublet pattern. IR measurements on the model molecule, **Ph-PERY-Ph**, indicated intermolecular hydrogen bonding induced by the carbamate linkage in solvents such as toluene, chloroform, and tetrachloroethane. UV and CD measurements confirmed the formation of aggregates in these solvents. The absence of a CD signal

and the absence of the aggregation peak in absorption spectra in THF indicated that the molecule was present in the molecularly dissolved state in this solvent. A dimeric structure has been proposed for the aggregate in solvents such as toluene, in which two perylene molecules are held together by intermolecular hydrogen bonding. Cyclic voltammetric measurements of **Ph-PERY-Ph** in CH_2Cl_2 unexpectedly had three reduction peaks. Assuming the presence of both the hydrogen-bonded and the non-hydrogen-bonded species in solvents such as $CHCl_3$, CH_2Cl_2, and tetrachloroethane, the new reduction peak can be expected to arise from the reduction of the hydrogen-bonded molecules. The redox behavior, good doping reversibility, quenching of fluorescence, and the formation of charge-separated states as indicated by the PIA spectra of **OPV-PERY-OPV**, indicate that this triad molecule could be a good candidate for solar cell devices.

Experimental Section

General procedures: 3,4,9,10-Perylenetetracarboxylic acid dianhydride, phenyl isocyanate, 20% solution of phosgene in toluene, and dibutyltin dilaurate were purchased from Aldrich and used without purification. The triad molecules, **OPV-PERY-OPV** and **Ph-PERY-Ph**, and all the intermediates were characterized by using a 400 MHz Varian NMR spectrometer in deuterated solvents, and TMS was used as internal reference. For samples recorded in $[D_2]$1,1,2,2-tetrachloroethane ($[D_2]$TCE), the solvent resonance was set to $\delta = 6.00$ ppm, and all other signals were referenced with respect to this peak. Similarly, for samples recorded in $[D_8]$tetrahydrofuran ($[D_8]$THF), the downfield solvent resonance was set to $\delta =$ 3.7 ppm, and all other signals were referred with respect to this peak. For the variable-temperature ^{1}H NMR measurements in $[D_2]$TCE, a minimum of 64 scans were signal averaged for each measurement, and the sample was allowed to equilibrate at the experimental temperature for 10 min prior to each measurement. For preparative size-exclusion chromatography, Bio-Beads S-X1 (mesh size 200–400, MW exclusion limit 14000) was used. Gel permeation chromatography (GPC) measurements were performed on a Waters 590 GPC using chloroform as solvent and a PL Gel column. An online UV/Vis detector ($\lambda = 254$ nm) was used and the instrument was calibrated by using polystyrene standards. MALDI-TOF mass spectra were recorded using a Perseptive Biosystems Voyager-DE PRO instrument in reflector mode with α-cyano-4-hydroxycinnamic acid as the matrix. Infrared spectra were recorded on a Perkin–Elmer Spectrum One instrument at a resolution of 4 cm^{-1} in a 0.5 μL cell. Absorption spectra were recorded by using a Perkin–Elmer Lambda 900 UV/Vis-NIR spectrophotometer. Circular dichroism (CD) spectra were recorded on a Jasco J-600 spectropolarimeter. The thermal characterization was carried out using a Perkin–Elmer differential scanning calorimeter Pyris 1 at a heating rate of 40 °C min^{-1}. Optical properties were studied using a Jeneval polarization microscopy equipped with crossed polarizers and a Linkam THMS 600 hot stage.

Cyclic voltammetry measurements: Cyclic voltammetry of the two molecules was measured in dichloromethane and tetrahydrofuran with 0.1M tetrabutylammonium hexafluorophosphate (TBAHF) as supporting electrolyte by using a Potentioscan Wenking POS73 potentiostat. The working electrode was a Pt disk (0.2 cm^2), the counter electrode was a Pt plate (0.5 cm^2), and a saturated calomel electrode was used as reference electrode against Fc/Fc^+. The scan rate was 100 mV s^{-1}.

***(E,E,E)*-4-{4-[4-(3,4,5-tridodecyloxystyryl)-2,5-bis[(*S*)-2-methylbutoxy]-styryl]-2,5-bis[(*S*)-2-methylbutoxy]styryl} phenyl isocyanate (3a)**: Compound **3a** was prepared starting from the aldehyde derivative.[20] The aldehyde was converted to the nitro derivative by a Wittig–Horner coupling reaction. This was reduced to the amine using $SnCl_2 \cdot 2H_2O$ and then converted to the isocyanate by using phosgene in toluene. (*E*,*E*,*E*)-4-{4-[4-(3,4,5-tridodecyloxystyryl)-2,5-bis[(*S*)-2-methylbutoxy]styryl]-2,5-bis[(*S*)-2-methylbutoxy]styryl} aniline (0.6 g, 0.46 mmol) was suspended in 20% phosgene solution in toluene (30 mL) and stirred at 95 °C for 15 h under argon. The complete conversion of the amine to the isocyanate was monitored by IR spectroscopy by observing the disappearance of the amine peak at 3364 cm^{-1} and the formation of the isocyanate peak at 2264 cm^{-1}. The reaction mixture was then cooled to room temperature and toluene removed in vacuo. Compound **3a** was used for the next step without further purification.

***N,N′*-Di-(1-isobutyl-2-hydroxyethyl)-3,4,9,10-perylene bis(dicarboximide) (4)**: (*S*)-(+)-Leucinol[21] (1.55 g, 1.32 mmol) was added to a solution of 3,4,9,10-tetracarboxyperylenedianhydride (1.7 g, 4.38 mmol) in freshly distilled quinoline (20 mL). The reaction mixture was heated at reflux for 24 h and subsequently cooled to room temperature. The solution was filtered and washed with dichloromethane. After evaporation of the dichloromethane, the product was precipitated with hexane to yield the title compound (2.43 g, 95% yield) as a dark red powder. ^{1}H NMR (300 MHz, $[D_8]$THF, 25 °C, TMS): $\delta = 7.99$ (m, 4H; ArH), 7.72 (m, 4H; ArH), 5.29 (m, 2H; −NC*H−), 4.25 (2H; OH), 4.07 (m, 2H; $-CH_2$), 3.80 (m, 2H; CH_2), 2.08 (m, 4H; CH_2), 1.59 (m, 4H; CH_2), 0.97 ppm (t, 12H; CH_3); MALDI-TOF MS (MW = 590.2): *m/z*: 590.5 $[M]^{+\cdot}$.

OPV-PERY-OPV: A solution of the isocyanate **3a** (0.60 g, 0.45 mmol) in dry methylene chloride was added to a solution of the *N,N′*-di-(1-isobutyl-2-hydroxyethyl)-3,4,9,10-perylene bis(dicarboximide) (**4**) (0.12 g, 0.21 mmol) in dry dichloromethane. Dibutyltin dilaurate (50 mg) was added as catalyst, and the reaction mixture was heated at reflux for 15 h at 55 °C under argon. The crude mixture was cooled to room temperature, the solvent was removed in vacuum, and the residue was then purified by silica gel chromatography with hexane as eluant. It was further purified using preparative size-exclusion chromatography (Bio-Beads) column with tetrahydrofuran as eluant to afford the title compound (0.16 g, 25% yield). M.p. 138 °C; ^{1}H NMR (400 MHz, $CDCl_3$, 25 °C, TMS): $\delta = 9.29$ (s, 2H; −NH−), 8.69, 8.19, 8.08, 7.76 (4 × d, 8H; perylene), 7.50 (s, 8H; Ar-H, vinylic H), 7.45–6.98 (m, 20H; Ar-H, vinylic H), 6.74 (s, 4H; Ar-H, vinylic H), 5.80 (m, 2H; −N−C*H−$CH_2(CH_2)$), 5.25 4.61 (m, 4H; −C*H−CH_2−OCO−), 4.03 (m), 3.86 (m, 28H; −OCH_2−), 2.28–0.89 ppm (m, 228H); ^{13}C NMR (100 MHz, $CDCl_3$, 25 °C): $\delta = 164.73$, 163.26, 153.74, 153.33, 151.24, 151.18, 151.14, 151.07, 138.26, 137.89, 133.84, 133.31, 133.16, 131.36, 131.04, 129.20, 128.64, 127.95, 127.50, 126.99, 126.86, 126.79, 125.49, 123.55, 122.64, 122.14, 118.92, 110.54, 109.94, 109.66, 105.18, 77.52, 77.29, 77.09, 76.67, 74.51, 74.26, 74.03, 73.62, 69.18, 53.48, 51.98, 38.03, 35.22, 35.16, 35.06, 32.01, 30.44, 29.84, 29.78, 29.74, 29.52, 29.47, 29.44, 26.45, 26.39, 26.21, 25.75, 23.17, 22.77, 22.64, 16.91, 16.85, 14.18, 11.57, 11.44 ppm; MALDI-TOF MS (MW = 3236): *m/z* : 3236.4 $[M]^{+\cdot}$.

Ph-PERY-Ph: Phenyl isocyanate (**3b**) (0.04 g, 0.36 mmol) in dry dichloromethane was added to a solution of **4** (0.11 g, 0.18 mmol) and dibutyltin dilaurate (40 mg) catalyst in dry dichloromethane. The solution was heated at reflux (55 °C) under argon for 15 h. The reaction mixture was cooled to room temperature, and the solvent was removed in vacuo to obtain a red pasty residue. This was stirred in hot hexane, filtered, and washed with hot hexane to remove traces of aniline. The red solid was then dissolved in CH_2Cl_2 and precipitated in cold methanol. Further purification by column chromatography on silica gel (ethyl acetate/hexane 1:4) gave the title compound (0.10 g, 65% yield). M.p. 240 °C; ^{1}H NMR (400 MHz, $CDCl_3$, 25 °C, TMS): $\delta = 9.10$ (s, 2H; −NH−), 8.64, 8.16, 7.99, 7.68 (4 × d, 8H; perylene), 7.49 (d, 4H; Ar-H), 7.22 (t, 4H; Ar-H), 6.99 (t, 2H; Ar-H), 5.75 (m, 2H, −N−C*H−$CH_2(CH_2)$), 5.19 (t) and 4.55 (dd) (4H; −C*H−CH_2−OCO−), 2.19 (m, 2H; −$CH(CH_3)_2$), 1.78, 1.53 (m, 4H; −C*H−CH_2−$CH(CH_3)_2$), 0.97 ppm (t, 12H; −CH_3); ^{13}C NMR (100 MHz, $CDCl_3$, 25 °C): $\delta = 164.72$, 163.38, 153.96, 138.78, 133.85, 133.47, 131.38, 131.07, 129.23, 129.03, 125.52, 123.63, 123.48, 123.36, 122.74, 122.32, 118.96, 65.37, 52.11, 38.13, 25.84, 23.26, 22.70 ppm; MALDI-TOF MS (MW = 828): *m/z* : 829.86 $[M]^{+\cdot}$.

[1] a) T. Tsuzuki, N. Hirota, N. Noma, Y. Shirota, *Thin Solid Films* **1996**, *273*, 177–180; b) M. Hiramoto, H. Kumaoka, M. Yokoyama, *Synth. Met.* **1991**, *91*, 77–79; c) J. J. Dittmer, E. A. Marseglia, R. H. Friend, *Adv. Mater.* **2000**, *12*, 1270–1274; d) K. Petritsch, J. J. Dittmer, E. A. Marseglia, R. H. Friend, A. Lux, G. G. Rozenberg, S. C. Moratti, A. B. Holmes, *Sol. Energy. Mater. Sol. Cells* **2000**, *61*, 63–72; e) J. J. Dittmer, R. Lazzaroni, Ph. Leclère, P. Moretti, M. Granström, K. Petritsch, E. A. Marseglia, R. H. Friend, J. L. Brédas, H. Rost, A. B. Holmes, *Sol. Energy. Mater. Sol. Cells* **2000**, *61*, 53–61.

  0947-6539/02/0815-3360 $ 20.00+.50/0 *Chem. Eur. J.* **2002**, *8*, No. 15

[2] a) J. F. Eckert, J. F. Nicoud, J. F. Nierengarten, S. G. Liu, L. Echegoyen, F. Barigelletti, N. Armaroli, L. Ouali, V. Krasnikov, G. Hadziioannou, *J. Am. Chem. Soc.* **2000**, *122*, 7467–7479; b) E. Peeters, P. A. V. Hal, J. Knol, C. J. Brabec, N. S. Sariciftci, J. C. Hummelen, R. A. J. Janssen, *J. Phys. Chem. B* **2000**, *104*, 10174–10190; c) L. H. Wang, Z. K. Chen, Y. Xiao, E. T. Kang, W. Huang, *Macromol. Rapid Commun.* **2000**, *21*, 897–900.
[3] C. J. Brabec, N. Saricifti, J. C. Hummelen, *Adv. Funct. Mater*. **2001**, *11*, 15–26.
[4] a) F. Würthner, C. Thalacker, A. Sautter, *Adv. Mater.* **1999**, *11*, 754–758; b) A. El-ghayoury, E. Peeters, A. P. H. J. Schenning, E. W. Meijer, *Chem. Commun*. **2000**, 1969–1970.
[5] a) G. R. J. Müller, C. Meiners, V. Enkelmann, Y. Geerts, K. Müllen, *J. Mater. Chem*, **1998**, *8*, 61–64; b) A. M. van de Craats, J. M. Warman, P. Schlichting, U. Rohr, Y. Geerts, K. Müllen, *Synth. Met.* **1999**, *102*, 1550–1551; c) M. Schneider, K. Müllen, *Chem. Mater*. **2000**, *12*, 352–362; d) M. Wehmeier, M. Wagner, K. Müllen, *Chem. Eur. J.* **2001**, *7*, 2197–2205.
[6] G. Seybold, G. Wagenblast, *Dyes Pigm*. **1989**, *11*, 303–317.
[7] D. Schlettwein, D. Wöhrle, E. Karmann, U. Melville, *Chem. Mater*. **1994**, *6*, 3–6.
[8] M. Sadrai, L. Hadel, R. R. Sauers, S. Husain, K. Krogh-Jespersen, J. D. Westbrook, G. R. Bird, *J. Phys. Chem.* **1992**, *96*, 7988–7996.
[9] M. P. O'Neil, M. P. Niemczyk, W. A. Svec, D. Gosztola, G. L. Gaines III, M. R. Wasielewski, *Science* **1992**, *257*, 63–65.
[10] a) D. Dotcheva, M. Klapper, K. Müllen, *Macromol. Chem. Phys.* **1994**, *195*, 1905–1911; b) H. Quante, Y. Geerts, K. Müllen, *Chem. Mater.* **1997**, *9*, 495–500.
[11] a) J. P. Meyer, D. Schlettwein, D. Wohrle, N. I. Jaeger, *Thin Solid Films* **1995**, *258*, 317–324; b) G. Hoprowitz, F. Kouki, P. Spearman, D. Fichou, C. Nogues, X. Pan, F. Garnier, *Adv. Mater*. **1996**, *8*, 242–244.
[12] L. Schmidt-Mende, A. Fechtenkötter, K. Müllen, E. Moons, R. H. Friend, J. D. Mackenzie, *Science* **2001**, *293*, 1119–1122.
[13] a) E. Hädicke, F. Graser, *Acta Cryst.* **1986**, *C42*, 189–195; b) E. Hädicke, F. Graser, *Acta Crystrallogr. Sect. C* **1986**, *42*, 195–198.
[14] C. Burgdorff, H.-G. Löhmannsröben, R. Reisfeld, *Chem. Phys. Lett.* **1992**, *197*, 358–363.
[15] F. Würthner, C. Thalacker, S. Dieke, C. Tschierske, *Chem. Eur. J.* **2001**, *7*, 2245–2253.
[16] R. A. Cormier, B. A. Gregg, *Chem. Mater*. **1998**, *10*, 1309–1319.
[17] a) V. L. Furer, *J. Mol. Struct.* **1998**, *449*, 53–59; b) V. L. Furer, *J. Mol. Struct.* **1999**, *513*, 1–8; c) V. L. Furer, *J. Mol. Struct.* **2000**, *520*, 117–123; d) M. M. Coleman, K. H. Lee, D. J. Skrovanek, P. C. Painter, *Macromolecules* **1986**, *19*, 2149–2157; e) K. Platteborze, J. Parmentier, Th. Z. Huyskens, *Spectrosc. Lett.* **1991**, *24,* 635–652; f) D. M. Mizrahi, H. E. Gottlieb, V. Marks, A. Nudelman, *J. Org. Chem.* **1996**, *61*, 8402–8406.
[18] P. Schouwink, A. H. Schäfer, C. Seidel, H. Fuchs, *Thin Solid Films* **2000**, *372*, 163–168.
[19] H. Langhals, *Heterocycles* **1995**, *40*, 477–500.
[20] A. P. H. J. Schenning, P. Jonkheijm, E. Peeters, E. W. Meijer, *J. Am. Chem. Soc.* **2001**, *123*, 409–416.
[21] H. Langhals, *Chem. Ber.* **1985**, *118*, 4641–4645.

Received: January 30, 2002 [F3842]